Enhanced Site Isolation in Cross-Link-Functionalized Polystyrene Networks: Mobility Studies Using Steady-State Fluorescence and ESR Techniques

Mark E. Wilson, Jennifer A. Wilson, and Mark J. Kurth*

Department of Chemistry, University of California, Davis, California 95616

Received October 23, 1996; Revised Manuscript Received March 6, 1997[⊗]

ABSTRACT: Enhanced site isolation and reduced site mobility have been demonstrated in polystyrene networks having trityl functionality at the cross-links through steady-state fluorescence measurements of intraresin excimer formation by 4-(1-pyrenyl)butanol labels and through ESR nitroxide spin-label studies. Suspension copolymerization of α,α-bis(4-vinylphenyl)benzyl alcohol with styrene afforded beads having trityl groups at the cross-links (C·Tr). Pendent-functionalized beads (P·Tr), prepared by copolymerization of α,α-diphenyl-4-vinylbenzyl alcohol with styrene and divinylbenzene served as a reference. Comparison of (I_e/I_m) as a function of polymer loading and solvent demonstrated that cross-link functionalization reduced site interactions, providing 30% higher effective dilution of labels. ESR of polymers labeled with 2,2,6,6-tetramethyl-4-oxopiperidin-1-oxyl oxime demonstrated C·Tr are less mobile than P·Tr. Possible origins of enhanced site-separation and reduced mobility are discussed and explored through various experiments.

One of the advantages associated with the use of polymeric supports is their ability to provide mutual separation between reactive sites. Polystyrene networks have been extensively investigated and reviewed[1−3] in this regard, and a number of factors have been found to influence site isolation. These include (1) degree of cross-linking, (2) concentration and distribution of functionality, (3) swelling, and (4) time frame. Permanent site separation has been demonstrated in resins containing >50% divinylbenzene,[4] but the mode of separation in lower cross-linked networks is predominantly kinetic. Although rapid reactions are an obvious prerequisite for kinetic site isolation, the diffusional characteristics of the support limit the effective "isolated" lifetime of reactive species. Increasing the cross-link density, while decreasing site-interactions through immobilization, unfortunately also results in acute diffusional limitations that cause slow and incomplete reactions. A particularly advantageous solution to this quandary would be to reduce the translational mobility of just the functional groups while retaining the diffusional properties of a lightly cross-linked network.

Our interest in solid-phase synthesis[5] and support modification[6] prompted us to investigate the efficacy of cross-link functionalization. Fluorescence depolarization[7] and neutron-scattering[8] studies on lightly cross-linked poly(dimethylsiloxane) (PDMS) networks have demonstrated that the translational mobility of cross-link junctions is more confined than that of chain ends or internal segments. With this in mind, we anticipated that cross-link-affixed trityl C·Tr (Scheme 1) would be less mobile than the corresponding pendant P·Tr. Pursuant of this, we introduced trityl groups at the cross-links of microporous beads by copolymerization of styrene with **2**. Pendent functionalized beads cross-linked to the same extent with divinyl benzene and having an equal amount of trityl functionality (via copolymerization of **1**) were prepared as a reference by which the effects of cross-link functionalization on site separation would be gauged.

Translational and rotational diffusion within the networks were measured by steady-state excimer fluorescence and electron spin resonance (ESR) nitroxide spin-label techniques, respectively. The excimer-to-monomer emission intensity ratio (I_e/I_m) of pyrenebutanol bound to the polymers via a trityl−ether linkage was used as a diagnostic of diffusion-controlled site interactions within the networks. The isotropic correlation times for rotational diffusion, determined through X-band ESR of 4-oxo-TEMPONE oxime-labeled polymers, provided a measure of the local segmental mobility (microviscosity) of the two types of attachment motifs. By comparing the influence of cross-link density, loading, and solvent upon translational and rotational diffusion, we sought to determine if cross-link functionalization decreases mobility and enhances site-separation, and if so, which parameters appear to augment the effect.

Scheme 1. Pendant (P·Tr)- and Cross-Link (C·Tr)-Functionalized Polystyrene Supports via Copolymerization

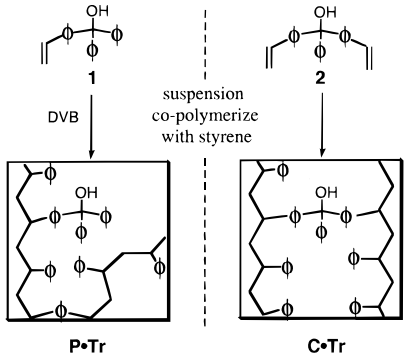

Materials and Methods

All reactions were performed in oven-dried (130 °C) glassware under a constant pressure of N_2. Solvents were purified prior to use except UV grade methanol, acetonitrile, dioxane, and pentane. Tetrahydrofuran and diethyl ether were distilled from sodium benzophenone ketyl. Methylene chloride was distilled from phosphorus pentoxide. Collidine was distilled from lithium aluminum hydride. Dimethylformamide was distilled from 4-Å molecular sieves. Chlorobenzene was distilled and stored under N_2. All reagents were used as received except potassium iodide (it was pulverized and dried overnight at 130 °C) and tetrabutylammonium perchlorate,

[⊗] Abstract published in *Advance ACS Abstracts,* May 15, 1997.

S0024-9297(96)01578-1 CCC: $14.00

which was dried for 48 h under vacuum in the presence of phosphorus pentoxide. Chromatographic separations employed 230−400 mesh silica gel (EM Sciences, Germany) and distilled hexanes−ethyl acetate. ^{1}H and ^{13}C NMR spectra were obtained with a General Electric QE-300 operating in pulsed Fourier transform mode. Infrared spectra were collected with a Galaxy 3000 FTIR (Mattson, Madison, WI) The mechanical motor used in suspension polymerization was a Janke and Kunkel IKA-WERK model RE 16 equipped with an RPM gauge IKA-TRON model DZM-1 (Staufen, Germany). The impeller and the 45/50 sealed shaft were also purchased from Janke and Kunkel.

α,α-Diphenyl-4-vinylbenzyl alcohol (1).[9] Into a dry 1 L flask were placed potassium (7.7 g, 197 mmol), anhydrous magnesium chloride (10.5 g, 110 mmol), potassium iodide (17.8 g, 107 mmol), and 300 mL of dry THF. The mixture was refluxed under N_2 for 3 h, giving a black precipitate (Mg^0), and allowed to cool to room temperature. 4-Bromosytrene (10.6 g, 58 mmol) was added dropwise over 4 h, and the reaction was stirred an additional 5 h at room temperature. A solution of benzophenone (10.7 g, 59.2 mmol) dissolved in 30 mL of THF was added dropwise and the reaction was stirred an additional 3 h. The solution was cooled to 0 °C, quenched with saturated ammonium chloride, and extracted with three 200 mL portions of diethyl ether. *tert*-Butyl catechol (5 mg, to inhibit polymerization) was added to the combined organic fraction, and the solvent was removed *in vacuo* to approximately 100 mL and dried with $MgSO_4$. Filtration and removal of the remaining solvent gave **1** as a light yellow solid that was purified by flash chromatography (5.68 g, 34.1%). Mp 74.5−75.2 °C. ^{1}H-NMR (300 MHz, $CDCl_3$) δ 2.7 (s, 1H, exchangeable with D_2O), 5.2 (dd, 1H, J = 10.5, 0.6 Hz), 5.7 (dd, 1H, J = 17.2, 0.7 Hz), 6.6 (dd, 1H, J = 17.6, 10.9 Hz), 7.1−7.3 (m, 14H). ^{13}C NMR (75 MHz, $CDCl_3$) δ 82.9, 114.0, 125.7, 127.2, 127.8, 127.9, 128.0, 128.5, 136.3, 144.1, 146.7. IR (KBr) 3465, 3060, 2925, 1008, 906 cm^{-1}. HR FAB-MS (matrix of 3-nitrobenzyl alcohol and poly(ethylene glycol): calcd for $C_{21}H_{18}O$, 286.1358; found, 286.1365.

α,α-Bis(4-vinylphenyl)benzyl Alcohol (2). The Grignard reagent from 4-bromostyrene (58 mmol) was prepared as for **1**, and then freshly distilled methyl benzoate (3.9 g, 29 mmol) was added dropwise and the reaction mixture was stirred for 3 h. The reaction was worked up as for **1** and purified by flash chromatography, affording **2** as a light yellow solid (3.23 g, 37%). Mp 91.8−92.4 °C. ^{1}H-NMR (300 MHz, $CDCl_3$) δ 2.7 (s, 1H, exchangeable with D_2O), 5.2 (dd, 2H, J = 10.9, 0.5 Hz), 5.7 (dd, 2H, J = 17.5, 0.6 Hz), 6.7 (dd, 2H, J = 17.6, 10.9 Hz), 7.2−7.4 (m, 13H). ^{13}C NMR (75 MHz, $CDCl_3$) δ 81.7, 114.1, 125.8, 127.3, 127.8, 128.0, 128.1, 136.3, 136.5, 146.3, 146.6. IR (KBr) 3461, 3085, 2923, 1006, 912 cm^{-1}. HR FAB-MS (matrix of 3-nitrobenzyl alcohol and poly(ethylene glycol)): calcd for $C_{23}H_{20}O$, 312.1514; found, 312.1520.

4-(1-Pyrenyl)butanol (3).[10] To a rapidly stirring solution of pyrenebutyric acid (Aldrich) (1.02 g, 3.55 mmol) in dry THF at 0 °C was slowly added lithium aluminum hydride (0.3 g, 7.9 mmol). The reaction was warmed slowly to room temperature with stirring for 3 h under N_2. The flask was placed in an ice bath, and 10 mL of 1 M NaOH(aq) was added dropwise to the solution with rapid stirring to afford a white-gray slurry that was filtered through a medium glass fritted funnel. The THF was removed *in vacuo*, and the crude product was taken up in diethyl ether and extracted 3 times with 50 mL of 0.1 M $NaHCO_3$(aq). The combined organic fraction was washed with brine, dried with $MgSO_4$, and concentrated to give a light brown oil that was purified by flash chromatography to give **3** as fine light brown crystals (0.97 g, 94%). Mp 79.3 −80.1 °C. ^{1}H-NMR (300 MHz, $CDCl_3$) δ 1.4 (s, 1H, exchangeable with D_2O), 1.7−1.8 (m, 2H, J = 7 Hz), 1.9−1.9 (m, 2H, J = 7 Hz), 3.4 (t, 2H, J = 7.8 Hz), 3.7 (t, 2H, J = 6.6 Hz), 7.9 (d, 1H, J = 9 Hz), 7.9 (q, 1H, J = 7.5 Hz), 8.0 (s, 1H), 8.1 (m, 5H, J = 8.5 Hz), 8.3 (d, 1H, J = 9.3 Hz). ^{13}C NMR (75 MHz, $CDCl_3$) d 27.8, 32.5, 33.0, 62.5, 123.3, 124.6, 124.7, 124.7, 124.8, 124.9, 125.7, 126.5, 127.2, 127.4, 128.5, 129.7, 130.8, 131.3, 136.5. IR (KBr) 3430, 3311, 3039, 2933, 2875, 1432, 843 cm^{-1}.

4-(1-Pyrenyl)butanol Trityl Ether (4). Into a 25 mL flask was added 4-(1-pyrenyl)butanol (108 mg, 0.39 mmol), chlorotriphenylmethane (151 mg, 0.54 mmol), collidine (157 mg, 1.3 mmol), and tetrabutylammonium perchlorate (21 mg, 0.06 mmol). Dry methylene chloride (15 mL) was added, and the solution was stirred at room temperature for 5 h. The solvent was removed *in vacuo*, and the crude material was purified by flash chromatography to give **4** as white crystals (0.161 g, 79%). Mp 126.4−128.4 °C. ^{1}H NMR (300 MHz, $CDCl_3$) δ 1.8 (p, 2H, J = 7.9 Hz), 1.9 (m, 2H), 3.1 (t, 2H, J = 6.3 Hz), 3.3 (t, 2H, J = 7.5 Hz), 7.3−7.2 (m, 10H), 7.5−7.4 (m, 5H), 7.8 (d, 1H, J = 7.8 Hz), 8.1−7.9 (m, 5H), 8.1 (d, 2H, J = 7.8 Hz), 8.2 (d, 2H, J = 9.3 Hz). ^{13}C NMR (75 MHz, $CDCl_3$) δ 28.4, 29.9, 33.2, 63.2, 86.4, 123.5, 124.6, 124.7, 125.0, 125.7, 126.5, 126.8, 127.1, 127.2, 127.5, 127.7, 127.9, 128.7, 128.8, 129.7, 130.9, 131.4, 136.9, 144.5. IR (film) 3054, 2931, 2867, 1509, 1448, 1072(br) cm^{-1}. HR FAB-MS (matrix of 3-nitrobenzyl alcohol and poly(ethylene glycol): calcd for $C_{39}H_{32}O$, 516.2453; found, 516.2469.

2,2,6,6-Tetramethyl-4-oxopiperidin-1-oxyl Oxime (5).[11] Into a 50 mL round bottom flask were added NH_2OH·HCl (1.41 g, 20.3 mmol), 5 mL methanol, and finely powdered KOH (1.3 g, 24.4 mmol). The slurry was stirred at room temperature for 15 min to free-base the hydroxylamine. The solution was filtered through a course fritted funnel into a 50 mL flask, and 4-oxo-TEMPO (Aldrich) (0.56 g, 3.31 mmol) was added with stirring at room temperature. The methanol was removed *in vacuo*, and the crude product was collected and recrystallized from anhydrous ethanol to give **5** as red crystals (0.42 g, 68%). Mp 163.8−164.6 °C. IR (KBr) 3334, 2992, 2940, 1658, 1463, 1332, 1136 cm^{-1}. HR FAB-MS (matrix of 3-nitrobenzyl alcohol and poly(ethylene glycol): calcd for $C_9H_{17}N_2O_2$, 185.1290; found, 185.1304.

Preparation of Functionalized Beads. Into a 250 mL Morton flask equipped with a side-arm (14/20 joint) condenser and an overhead stirrer were placed 100 mL of Millipore water along with gum arabic (6 g). The solution was degassed by purging with N_2 while heating at 90 °C for 30 min with rapid stirring. The monomer mixture (*vide infra*) containing benzoyl peroxide (0.1 g) and chlorobenzene (10 g) was added, and the stirring rate was adjusted to 450 rpm. After 15 min, finely pulverized aluminum oxide (0.1 g, acidic) was added to stabilize the suspended droplets. The system was kept at 90 °C under N_2 for the duration of the polymerization (24 h). The beads (yield 88−99%) were poured into a 300 mL course fritted funnel and washed with 100 mL of 0.5 M aqueous HCl to remove the aluminum oxide. The beads were washed with 100 mL each of H_2O, 50:50 THF−H_2O, THF, and ether. Sizing was done by passing an ethanolic slurry of the beads through Teflon meshes (Spectrum, Houston, TX) from 105 to 300 μM. The beads were rinsed with diethyl ether and petroleum ether and then dried overnight in a vacuum oven at 45 °C.

Table 1. Representative Formulations

polymer[a]	monomer[b] (g)	styrene (g)	DVB[c] (g)
2-P·Tr	0.43	9.23	0.35
4-P·Tr	0.83	8.49	0.67
8-P·Tr	1.58	7.15	1.27
2-C·Tr	0.47	9.53	
4-C·Tr	0.91	9.09	
8-C·Tr	1.73	8.27	

[a] Number preceding descriptor corresponds to % (w/w) DVB to achieve X_c. [b] **1** for P·Tr, **2** for C·Tr. [c] Technical grade DVB.

Polymer Formulations. The cross-linker in the C·Tr series was **2**, but in the P·Tr series it was technical grade divinylbenzene (DVB) containing 56% of a mixture of 3,4-isomers (the balance is mostly ethylvinylbenzene, EVB). We accounted for the presence of EVB by adding more technical grade DVB such that the mole percent of cross-linker (X_c) was identical in both types of polymers. Also, we kept the trityl loadings similar for the same X_c. Thus, the amount of monomer **1** in the P·Tr resins was adjusted accordingly. Representative formulations are listed in Table 1.

Polymer-Bound 3. Polymer (4 g), along with phosphorus pentachloride (2 g, 50 equiv), was suspended in methylene chloride and refluxed without a stir bar for 48 h. The beads were extracted with THF for 48 h and allowed to dry in a

vacuum dessicator. Samples were titrated for chlorine content with silver nitrate.[12] Polymers (200 mg) were placed into 5 mL screw-cap vials. A standard solution of **3** in dry methylene chloride (containing 10% methanol) was added such that the loading was varied from 0.1 mmol to the maximum possible given the trityl chloride content. Dry collidine (2 mmol for every mmol of **3**) and tetrabutylammonium perchlorate (0.1 mmol for every mmol of **3**) were added, and the vials were purged with N_2, sealed, and placed on a rotating carousel (J. A. G. Industries, Baltimore, Maryland) for 7 days. The beads were extracted with THF for 48 h and dried for 12 h in a vacuum oven at 35 °C.

Polymer-Bound 5. Chlorinated polymer (200 mg) was loaded with oxime **5** according to the same procedure as with **3** except that, instead of methanol being added to assist in a more homogeneous distribution of labels, it was cyclopentanone oxime. Thus, separate solutions of **5** and cyclopentanone oxime (Aldrich) in methylene chloride (1.55×10^{-3} M) were prepared. Aliquots of the stock solutions were added to the beads such that the loading of **5** was held below 0.05 mmol/g while the total millimoles of oxime (**5** + cyclopentanone oxime) was equal to the maximum theoretical loading of the given polymer.

UV-Loading Assays. Polymer beads labeled with **3** (5 mg) were placed into a preweighed screw-cap vial (2×7 cm^2) along with 15 mL of stock solution of trifluoroacetic acid in chloroform (1:50). The beads immediately turned red (trityl cation), releasing **3**. The vials were capped, covered in foil, and placed on a rotating carousel for 4 h. The vials were weighed, small aliquot was transferred into a 3 mL UV cuvette, and the absorbances at 314, 328, and 345 nm (against the 1:50 TFA−$CHCl_3$ background solution) were taken in triplicate using a Hewlett-Packard 8450A UV−vis spectrophotometer. The concentrations of the solutions were calculated from three separate standard curves (at each wavelength). The loading was then determined from the total mass of analyte solution (total mmol of **3**) and the polymer mass. Each polymer was assayed in at least triplicate.

Fluorescence Measurements. Spectra were collected with a Perkin Elmer LS 50B luminescence spectrometer with the excitation slit set at 2.5 nm, and the emission slit was varied to achieve a constant signal maximum. Excitation wavelengths were varied as discussed. Polymer samples were prepared by placing the beads (10 mg) in small screw-cap vials with freshly distilled solvent for 24 h prior to collection. A small slurry of beads (~3 mg) was added to a standard 3 mL fluorescence cuvette, and the sample was degassed by a stream of nitrogen for 30 s and then placed in the beam such that emission was observed. All spectra (collected in at least triplicate) were uncorrected. Baseline corrections for the small background emission of polystyrene were not performed (the subtraction had a negligible effect upon the value of I_e/I_m). All spectra were normalized at 397.5 nm.

Electron Spin Resonance (ESR). X-band spectra were acquired with a Varian E-4 EPR spectrometer operating in continuous wave mode at a frequency of 9.5 GHz. Scan ranges were 100 G for full spectra and 10 G for measurement of central hyperfine line widths. Power varied from 11.5 to 20 dB, depending upon signal strength. Modulation amplitude and frequency were held at 4 G and 100 Hz, respectively. Polymer samples (50 mg) were placed in a 4 mm (i.d.) quartz tube. Degassed solvent was added, and the tube was flushed with N_2 for 10 min, sealed, and allowed to stand for 5 h prior to data collection. Spectra were collected at room temperature (23−25 °C) over 8−16 min using a time constant of 0.3−1.0 s, respectively.

Line Width Analysis. Isotropic correlation times were calculated according to the method of Goldman.[13] In the motionally narrowed regime ($0.04\tau < 2$ ns), the expression for correlation time τ becomes

$$\tau = \frac{15B}{8\pi\omega g(0)\, D(0)} \tag{1}$$

where ω is the instrument operating frequency (in rads/s), the spherical tensor components are

$$g(0) = (1/\sqrt{6})[2g_{zz} - (g_{xx} + g_{yy})],$$
$$D(0) = (1/2\sqrt{6})[2A_{zz} - (A_{xx} + A_{yy})]$$

and B is the isotropic line shape parameter:

$$B = \frac{\sqrt{3}}{4}\Delta H(0)_c\left[\sqrt{\frac{V(0)}{V(+1)}} - \sqrt{\frac{V(0)}{V(-1)}}\right] \tag{2}$$

The values for the g-tensors of nitroxide **5** were assumed to be the same as those of the parent compound TEMPONE ($g_{xx} = 2.0104$, $g_{yy} = 2.0074$, $g_{zz} = 2.0026$).[14] Because exact values for the A-tensors in various solvents are not known, these were estimated by using the identity

$$a_n = {}^1/_3(A_{xx} + A_{yy} + A_{zz}) \tag{3}$$

Assuming $A_{xx} \approx A_{yy}$, and substituting the A_{zz}-tensor of TEMPONE[15] (31 G) along with the nitrogen hyperfine splitting constant a_n of TEMPONE in the given solvent[16] gives an estimation of the A-tensors.

The values in eq 2 were taken from the first derivative spectra. $V(0)$ is the peak- to-peak height of the central ($m = 0$) hyperfine line, and $V(\pm1)$ are the peak-to-peak heights of the $m = \pm1$ lines. The central hyperfine peak-to-peak width $\Delta H(0)$ contains some errors (<10%) caused by Gaussian inhomogeneous line broadening. A method developed by Bales using the relation[17]

$$\Delta H(0)_c = \Delta H(0) - \frac{(Da_n + E)^2}{\Delta H(0)} \tag{4}$$

where D and E have the values[18] −0.1232 and 2.202, respectively, was used to correct for this.

Results and Discussion

Steady-State Excimer Fluorescence. Excimer fluorescence has been widely used to characterize diffusion and specific molecular interactions within polymers.[19,20] The formation of intra- and intermolecular excited state dimers of pyrene groups attached to polymers has been used to provide information about morphology,[21] microviscosity[19] and macrocyclization in both linear[22,23] and cross-linked[24] polymers. Considering the sensitivity and experimental practicality of steady-state excimer fluorescence, we were surprised that there are no reports of this technique as a diagnostic of site isolation in polymeric supports. In addition, because excimer formation is a diffusion-controlled process[25] involving the interaction of transient species (excited states), it provides a look into the kinetic aspects of site isolation with minimal perturbation of the system in a manner that closely mimics the dynamics of reactive intermediates involved in synthesis.

Scheme 2 illustrates how we attached pyrene via 4-(1-pyrenyl)butanol (**3**) to the cross-link and pendent functionalized resins. The emission spectrum of polymer-bound **3** (Figure 1) exhibits two bands corresponding to the isolated pyrene (397.5 nm) and the excimer (474 nm). Although the Stoke's shift remained essentially constant for all spectra, the relative intensities of the monomer (I_m) and excimer (I_e) varied considerably with polymer loading and excitation wavelength. The dependence on excitation wavelength could be negated by holding λ_{excit} constant, but it was impossible to exactly match the loading of each polymer. Thus, we varied the loading of each polymer and constructed a calibration curve of I_e/I_m versus loading (as determined by release/UV-assay). The direct comparison of the poly-

Scheme 2. Preparation of Pyrene-Labeled Polymers and Solution Reference Probe 4

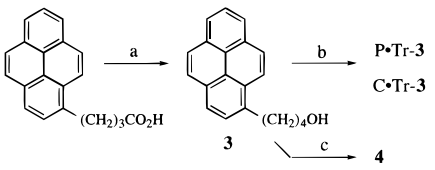

(a) $LiAlH_4$, THF. (b) P•Tr-Cl or C•Tr-Cl, CH_2Cl_2, Bu_4ClO_4, collidine. (c) Trityl chloride, CH_2Cl_2, Bu_4ClO_4, collidine.

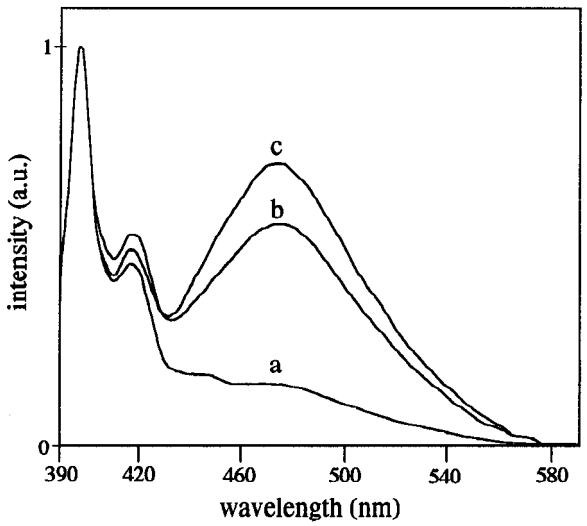

Figure 1. Representative emission spectrum of pyrene label **3** bound to 6% cross-linked C•Tr in THF with the following loadings: (a) 0.068, (b) 0.174, and (c) 0.22 mmol/g. Excitation wavelength 350 nm, with normalization at 397.5 nm.

Scheme 3. Kinetic Model for Intraresin Excimer Formation (Py = Pyrene Label 3)

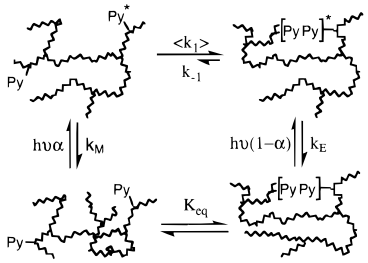

mers at constant loading was made possible by calculating the value of I_e/I_m at a set value.

Mechanistic Considerations of Excimer Fluorescence. A pyrene excimer, as defined by Birks,[26] requires the encounter of a localized electronically excited pyrene with a second ground-state pyrene forming a sandwich-like complex (interchromophore separation is typically in the range 3−3.7 Å).[27] This type is referred to as a "dynamic" excimer. The formation of dynamic excimers is widely considered to be a diffusion-controlled process.[28] A second type of excimer can form when pyrene groups are preassociated and the pair become excited. This type is termed a "static" excimer. Scheme 3 shows the mechanism of excimer formation in labeled polymers[29] adapted to a network. Here, we neglect multiple or augmented excimer populations arising from singlet-energy transfer or differences in conformational populations,[30] as we believe these problems are minimized in our study. The facile excimer-forming properties of pyrene along with the low loadings minimize singlet-energy transfer, and the long lifetime of the pyrene excited state (≈200 ns) ensures that local

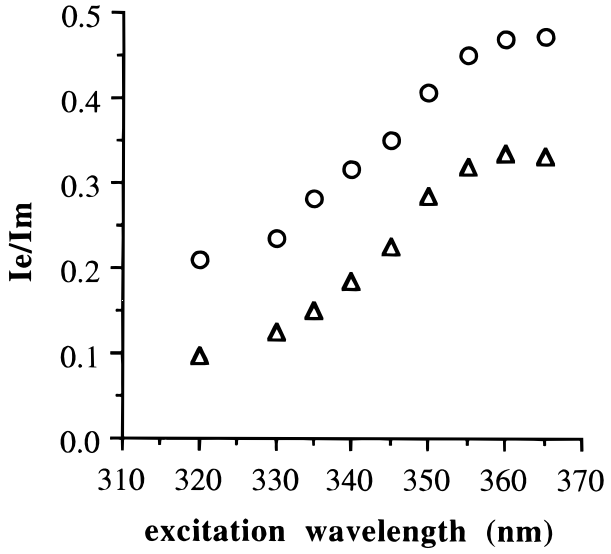

Figure 2. Effect of excitation wavelength on the I_e/I_m ratio of 6% cross-linked P•Tr (○) and C•Tr (△) in methylene chloride. Loadings are 0.071 and 0.068 mmol/g, respectively.

conformational changes will most likely be averaged so that the geometrical requirements for excimer formation will be met more or less equally.

According to the kinetic model, k_E represents the sum of radiative (k'_E) and non-radiative decay of the excimer and k_M is the sum of radiative (k'_M) and nonradiative decay of monomeric pyrene. The term $\langle k_1 \rangle$ represents the diffusion-controlled (encounter controlled) rate constant for dynamic excimer formation with the brackets indicating the rate constant is for an ensemble of labels separated by various chain lengths. Excimer dissociation is described by the term k_{-1}. Equilibration of ground-state pyrenes to associated ground-state dimers is given by K_{eq}, with α corresponding to the fraction of light absorbed by nonassociated chromophores. At room temperature, the value of k_{-1} is ca 20% that of k_E[23] and under some circumstances (system dependent) negligible in comparison to $\langle k_1 \rangle$.

While meaningful values for the kinetic constants in Scheme 3 can only be obtained through time-resolved techniques, steady-state fluorescence measurements can provide information about both dynamic and static excimer formation. Figure 2 shows the increase in I_e/I_m with excitation wavelength for 6% cross-linked P•Tr and C•Tr in methylene chloride. In the longer wavelength region, I_e/I_m increases as a consequence of the ($S_1 \leftarrow S_0$) transition of isolated pyrene being forbidden, with very low extinction coefficients (ϵ < 600 L mol^{-1} cm^{-1} in cyclohexane).[29] In the lower wavelength regime, absorption by the static dimers is minimal and the I_e/I_m ratio is predominantly a measure of dynamic excimer formation. Thus, at lower wavelengths, I_e/I_m can be correlated to the kinetics of dynamic excimer formation through the expression[31]

$$\frac{I_e}{I_m} \approx Q\frac{k'_E}{k'_M}\left(\frac{[M]\langle k_1 \rangle}{k_{-1} + k_E}\right) \qquad (5)$$

where Q relates I_e/I_m to the quantum efficiencies of excimer and monomer and [M] is the local concentration of pyrene labels. For similar polymers in the same solvent where Q and (k_{-1} + k_E) do not vary,[32] the expression becomes[33]

$$\frac{(I_e/I_m)_1}{(I_e/I_m)_2} \approx \frac{(\langle k_1 \rangle)_1}{(\langle k_1 \rangle)_2} \frac{[M]_1}{[M]_2} \quad (6)$$

Comparison of the normalized intensity ratios $(I_e/I_m)_1$ and $(I_e/I_m)_2$ of the P·Tr and C·Tr polymers, respectively, gives a qualitative measure of the effects of local pyrene concentration and translational diffusion upon site-separation. That this approach reflects primarily the kinetic aspects of site-interations is supported by the dependence of both I_e/I_m and $<k_1>$ on interlabel chain length, solution viscosity, and chain solvation.[34]

Results of Fluorescence Measurements. The loading versus I_e/I_m calibration curve for 6% cross-linked P·Tr- and C·Tr-labeled polymers in THF is shown in Figure 3. The increase in excimer formation with loading is a reflection of an increase in the local chromophore concentration. While the linearity of the plots concurs with our kinetic model, it is interesting that the slopes are similar. If there are significant differences between the kinetic parameters of excimer formation within the P·Tr and C·Tr networks, it is likely they would manifest themselves here. The most significant feature of the plot, however, is that the C·Tr-bound labels display consistently *less* excimer formation than those bound to P·Tr. At a loading of 0.15 mmol/g, the C·Tr polymers have a I_e/I_m ratio of 0.33 while the P·Tr show a value of 0.49.

The I_e/I_m ratios at 0.15 mmol/g for both series of labeled polymers (Figure 4) indicate that at all cross-link densities C·Tr displays less excimer formation than P·Tr. Whilst the differences remain essentially constant through 4−8% cross-linking, the polymers display more similar I_e/I_m ratios in the higher cross-linked regime. Interestingly, the 8−13% cross-linked C·Tr show very similar I_e/I_m ratios but the corresponding P·Tr series differ considerably.

One possible origin of the reduced I_e/I_m ratios observed in C·Tr relative to P·Tr could be a disparity in the distribution of chromophores in the two polymer networks. While the distribution of trityl groups within each network was set by the reactivity ratios of the respective monomers during copolymerization, the distribution of pyrene labels was a function of the relative accessibility and reactivity of the polymer-bound trityl chloride. Copolymers of styrene and DVB are known to be heterogeneously cross-linked,[35] and unless C·Tr is similar in this respect, it is likely that the structures of the networks will differ. Such differences are known to have profound effects upon site accessibility and reactivity.[36] We attempted to address these potential differences by adding a small aliquot of methanol to compete with **3** for sites. However, there is no way of knowing the extent to which this achieved an equal distribution of labels within the two networks.

Another possible origin of the reduced I_e/I_m ratios in C·Tr is that they are more sterically crowded than P·Tr. Because the pyrene labels were bound to the sites by only a four-carbon linker, it is conceivable that steric interactions could reduce excimer formation and even distort excimer geometry. Farid and co-workers, studying the effects of glassy polymer hosts on the spectral properties of 4-(1-pyrenyl)butyrate, attributed a blue shift in the excimer emission (35 nm in PS) to a distortion of the excimer geometry.[37] The emission spectrum of dry 4% cross-linked C·Tr and P·Tr at 100 °C revealed that the polymer-bound excimers had similar maxima occurring at 476 and 473 nm, respectively.[38] These were very similar to the values observed in the solvent-swollen polymers (474 ± 4 nm). If there are steric influences, they do not appear to manifest observable distortions in excimer geometry.

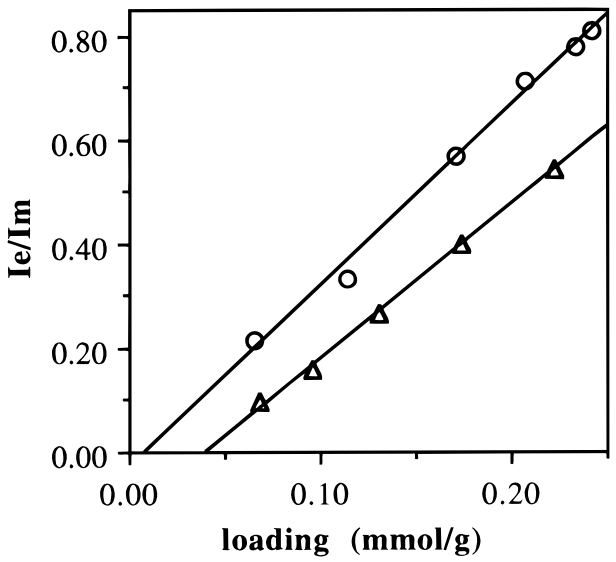

Figure 3. I_e/I_m ratio of labeled 6% cross-linked P·Tr (○) and C·Tr (△) in THF at various loadings of pyrene label **3**. λ_{excit} = 340 nm. Intensities normalized at 397 nm. Loading of **3** determined by release-UV assay.

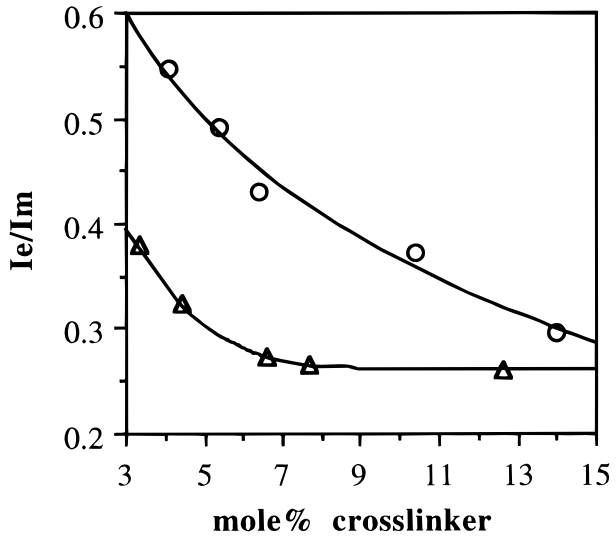

Figure 4. Extrapolated I_e/I_m ratios of P·Tr (○) and C·Tr (△) in THF. Loading of **3** set at 0.15 mmol/g with values taken from a series of four- to six-point calibration curves like Figure 3.

Our initial hypothesis was that C·Tr would exhibit lower I_e/I_m ratios because they possessed less mobility than P·Tr. Unfortunately, the differences in the microstructure of the networks arising from the use of very different cross-linking agents precludes the unambiguous assignment of the origin of reduced excimer emission in C·Tr. Specifically, differences in the reactivity of DVB relative to **2** likely resulted in a different distribution of cross-links within the two networks. The lengths of chains between junctions are known to influence the dynamics of networks,[39] and the universal square-root dependence of the chain constraint constant (a measure of network tendency toward affine versus phantom behavior) with network chain length[40] infers that these differences could influence translational diffusion.

While there is no way of measuring diffusional processes (e.g., dynamic excimer formation) to the

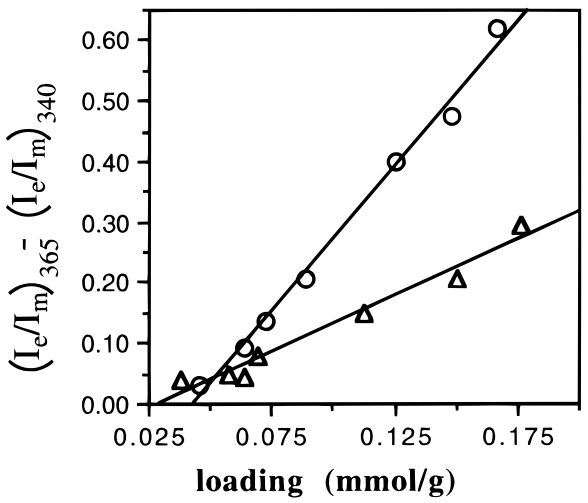

Figure 5. Relative increase in I_e/I_m as a function of polymer loading for 4% cross-linked P·Tr (○) and C·Tr (△) in methylene chloride.

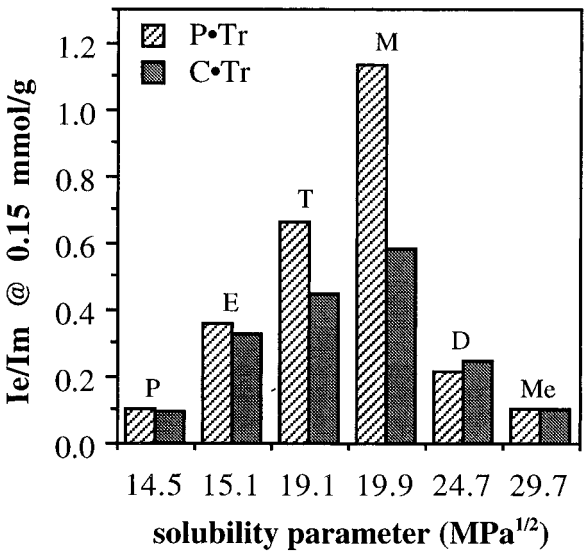

Figure 6. Influence of solvents *n*-pentane (P), Et_2O (E), THF (T), CH_2Cl_2 (M), DMF (D), and methanol (Me) upon I_e/I_m; λ_{excit} = 350 nm; solubility parameters taken from ref 46.

exclusion of preassociative processes (static excimers) using steady-state techniques, it is possible to gain insights into their relative contributions. In the limiting case of low excitation wavelengths, the majority of I_e is attributed to dynamic excimers. Consequently, Figures 3 and 4 reflect the diffusional (kinetic) aspects of site-separation within the networks. Insights into the extent of preassociated pyrene labels can be achieved by examining the dependence of I_e/I_m on excitation wavelength. The value of I_e/I_m increases with excitation wavelength primarily because monomeric excitation is reduced. The I_e/I_m ratio can also be enhanced by the formation of preassociated pyrene dimers that absorb >350 nm. Thus, an increase in the response of I_e/I_m with increasing excitation wavelength reflects an increase in preassociation.

Figure 5 shows the relative response of I_e/I_m at "monomer" excitation (λ_{excit} = 340 nm) and "dimer" excitation (λ_{excit} = 365 nm) as a function of polymer loading in 4% cross-linked C·Tr and P·Tr. The amount of preassociated dimer can be seen to increase as a function of loading in both polymers, as evidenced by the increasing difference between $(I_e/I_m)_{340}$ and $(I_e/I_m)_{365}$. Most notable is the greater response of P·Tr over C·Tr, suggesting that there is more preassociation within the P·Tr network for the same overall loading and that a change in loading has a greater effect upon preassociation. While the electronic stabilization of the pyrene excimer is substantial (ΔH = 10 kcal mol^{-1}),[41] there is also evidence of a small favorable interaction between ground-state pyrenes.[42] Thus, the markedly increased response of P·Tr to an increase in loading may be a reflection of a higher K_{eq} value. Alternatively, the distribution of functionality within P·Tr may be more aggregated than that of C·Tr, making the effect of an overall increase in pyrene loading more pronounced. Preassociated dimers or aggregates have been observed in LB thin films[43] and end-labeled PEO.[44] The markedly reduced response of C·Tr to an increase in loading suggests that preassociation via dimer or aggregates is substantially less in the cross-link functionalized network.

The influence of solvent upon I_e/I_m (Figure 6) was profound. In poor solvents, excimer formation is reduced, but in good solvents I_e/I_m is increased. Polymer−solvent compatibility (gauged by the solubility parameter) appears to influence excimer formation, as evidenced by the higher I_e/I_m ratios occurring at 19.9 MPa$^{1/2}$. This is slightly higher than the value of polystyrene (widely reported as 18.6 MPa$^{1/2}$)[45] but still within the range of "good" solvents (±1.8). Interestingly, the largest difference between the polymers also occurs here. In methylene chloride, the I_e/I_m ratio for P·Tr is 1.13, nearly twofold higher than that for C·Tr! While the exact origin of this large increase is unknown, it is consistent with the behavior of a nonuniformly cross-linked network. Introduction of a large excess of "good" solvent into a gel causes excluded volume interactions between the chains, resulting in overswelling. If the cross-linking in the P·Tr network is inhomogeneous (i.e., more dense regions are present where the chains are already in their optimal excluded volume conformations), swelling of these microregions would be minimal because it requires real stretching of the chains—an unlikely event given the energetic cost. This would mean that the majority of overswelling would be accounted for by the chains within the interstitial (between clusters) regime. Functionality bound to these chains (i.e., P·Tr) would exhibit a higher level of excimer formation by virtue of increased mobility. That the C·Tr were markedly less sensitive to changes in solvent suggests either that the cross-linking within the C·Tr is more uniform than that in P·Tr or that functional group mobility is less dependent upon polymer−solvent interactions.

Overall, the response of each gel to changes in solvent was larger than the differences between the gels in a given solvent. Even a switch in the relative order of I_e/I_m can occur. In DMF, C·Tr exhibits more excimer formation than P·Tr. This observation, incidentally, casts some doubt upon the idea that C·Tr are more sterically crowded than P·Tr. The response of the polymers differs radically, however, from that of end-labeled linear polystyrenes, which display *lower* I_e/I_m ratios in good solvents.[31] Thus, it is unlikely that diffusion within these networks is influenced by excluded volume effects to the same extent as in linear systems. Moreover, the major factor influencing excimer formation appears to be the solvating power of the solvent.

From the perspective of site isolation synthesis, we were interested in the "dilution" associated with poly-

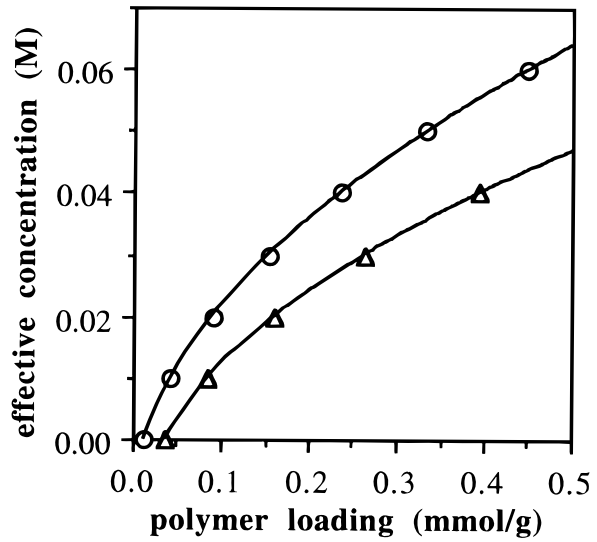

Figure 7. Effective concentration of pyrene bound to P·Tr (○) and C·Tr (△) in methylene chloride. Concentrations derived from the corresponding I_e/I_m ratios observed in solution phase **4**.

mer immobilization. Comparison of the I_e/I_m ratio observed for polymer-bound **3** as a function of loading with the I_e/I_m ratio of solution phase **4** as a function of concentration provides a qualitative measure of the effective polymer concentration. Pursuant to this, a calibration curve relating I_e/I_m to the concentration of **4** in methylene chloride was constructed. Setting the observed I_e/I_m of the labeled polymers in methylene chloride to that of solution phase **4** and solving for the concentration of **4** gives an "effective concentration" (Figure 7). While 6% cross-linked C·Tr provides slightly more "dilution" than the corresponding P·Tr, the advantage is modest. At an equal loading of 0.4 mmol/g, C·Tr give an effective concentration of 0.04 M and P·Tr afford dilution to 0.05 M, a 30% increase in concentration. Although this estimation is valid only for pyrene excimer formation, it is reasonable that there may be a measurable increase for other processes under kinetic control. The I_e/I_m ratios used to construct the effective dilution curve in Figure 7 were collected at an excitation wavelength of 350 nm. Consequently, they reflect both diffusion and preassociation. Reactions occurring within polymer supports will vary greatly in terms of the relative amount of preassociation and reaction rate. With this in mind, our estimation is that only very rapid reactions having little preassociation will actually benefit from cross-link functionalization.

ESR Nitroxide Spin-Label Studies. The mobility of functional groups bound to network polymers can be examined by ESR. Attachment of a nitroxide spin label and analysis of the hyperfine lines of first derivative spectra afford information about the correlation time for rotational diffusion.[46] Isotropic correlation time (τ), defined as the time required for the nitroxide to rotate through an angle of 1 rad, is inversely proportional to mobility. In labeled polymers, it has been shown to be a measure of the mobility of chain segments.[47,48] Both cross-link density[49] and polymer swelling[50] have profound effects. Regen, for example, found that polystyrene resins labeled with 4-hydroxy-2,2,6,6-tetramethylpiperidin-1-oxyl exhibited longer isotropic correlation times in poor swelling solvents and shorter times in better swelling solvents.[51]

We attached the nitroxide 2,2,6,6-tetramethyl-4-oxopiperidin-1-oxyl oxime (**5**) via a trityl ether linkage to

Scheme 4. Preparation of Nitroxide Spin Label 5 and Attachment to the Polymers

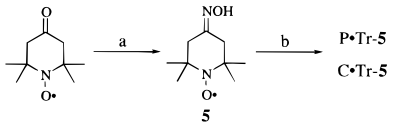

5

(a) $HONH_2$•HCl, KOH, CH_3OH. (b) P•Tr-Cl or C•Tr-Cl, CH_2Cl_2, Bu_4ClO_4, collidine; loading of **5** < 0.05 mmol/g by competative loading with cyclopentanone oxime.

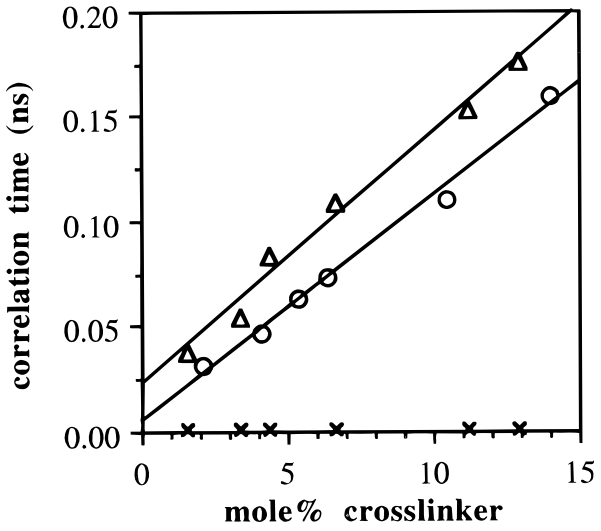

Figure 8. Isotropic correlation time of P·Tr (○), C·Tr (△), and solution phase **5** (×) in CH_2Cl_2.

a series of P·Tr and C·Tr resins of varying cross-link density (Scheme 4). Loadings were kept low to avoid dipole−dipole interactions between labels, and concomitant attachment of cyclopentanone oxime ensured a more homogeneous distribution of the labels throughout the polymers.

Figure 8 shows the isotropic correlation times of spin-labeled C·Tr and P·Tr networks of varying cross-link density. Immobilization of **5** to the polymers can be seen to increase the isotropic correlation times relative to those for the freely solvated nitroxide, with greater immobilization affected by increasing X_c. The salient feature of the plot, however, is that C·Tr have consistently higher correlation times than P·Tr. While the differences are modest, the trend suggests placement of functionality at the cross-link reduces mobility. That this mobility is of a local nature is inferred from ESR studies of linear polymers that displayed an increase in τ with molecular weight to limiting values within five monomer units, suggesting short range segmental motion is the dominant factor.[52]

The influence of solvent on site mobility is quite obvious in the first derivative spectra (Figure 9). In methylene chloride, the hyperfine lines of spin-labeled C·Tr appear relatively narrow, but in diethyl ether the lines become broader. In the poor solvent acetonitrile, the spectrum appears to take on some of the features of the nitroxide powder spectrum. This effect was also observed in the P·Tr networks, as the correlation times given in Table 2 indicate. Most notable are the significantly higher correlation times in the poor swelling solvents pentane and methanol. Although these values exceed the regime in which motionally narrowed linewidth analysis is accurate[53] (in fact, calculations of τ in acetonitrile were not possible), both polymers appear to have, at least qualitatively, the same immobility. In solvents that swell the polymers, correlation times are significantly lower. This behavior may be interpreted

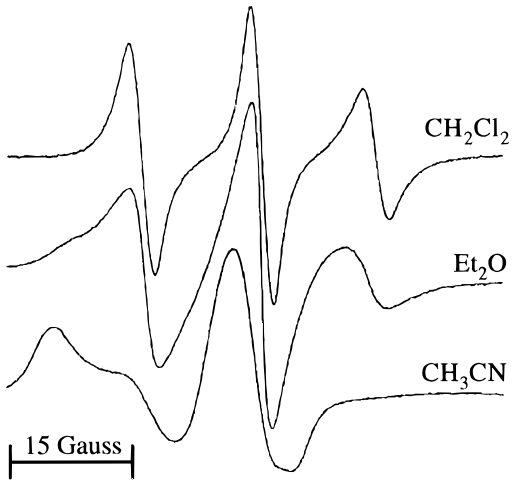

Figure 9. Influence of solvent upon the first-derivative ESR spectrum of 6% cross-linked C·Tr−**5** in various solvents.

Table 2. Effect of Solvent on Correlation Time

	correlation time (ns)	
solvent	P·Tr	C·Tr
methanol	2.51	2.54
dimethylformamide	0.144	0.104
methylene chloride	0.089	0.092
tetrahydrofuran	0.103	0.107
diethyl ether	0.246	0.290
dioxane	0.216	0.245
n-pentane	2.55	2.53

in terms of polymer−solvent interactions. In poor solvents the polymer chains assume a more tightly coiled structure, leading to an increase in the intrachain steric interactions opposing segmental motion.[54] In good solvents the polymer coils are expanded enough to allow for more rapid segmental motion.

The influence of solvents, as measured through ESR, indicated the same qualitative trends as the fluorescence measurements indicated. Functional group mobility is increased in good solvents and decreased in poor solvents. As in the fluorescence data, ESR indicated that the labels had the most mobility in methylene chloride and the least in methanol, pentane, and acetonitrile. Interestingly, in the same solvent that produced lower eximer formation in P·Tr relative to C·Tr, a similar reversal was noted in the correlation time. In dimethylformamide, P·Tr exhibits a higher correlation time than C·Tr. With the overall similarities between the two diagnostics, it was tempting to suggest an inverse relationship between I_e/I_m and τ. Indeed, with the known inverse dependence of excimer formation on solvent viscosity η[55] and the direct correlation between τ and viscosity indicated by the Stokes−Einstein relation

$$\tau = K\eta/T \qquad (7)$$

where T describes the influence of temperature, and one may expect a linear correlation. Inspection of the values in Figure 6 and in Table 2, however, reveal that there is poor correlation. Presumably, the scope of the spin-label technique, being more a measure of local mobility, is somewhat narrower than excimer fluorescence. Thus, we suggest that excimer fluorescence, because it relates more directly to translational diffusion, and site-interactions (as opposed to an inferred relationship between mobility and diffusion) is a more reliable diagnostic of site isolation within polymer networks.

Summary

Placement of functionality at the cross-links of microporous polystyrene appears to enhance site isolation, as evidenced by an overall reduction in the I_e/I_m ratio relative to those for P·Tr networks. These results were corroborated by longer isotropic correlation times in spin-labeled C·Tr relative to P·Tr. The differences between the polymers were greatest when the cross-link densities were below 8% and the beads were in the presence of good swelling solvents. While the exact origin of the enhanced site-separation in C·Tr is not clear, we suspect it is a combination of sterics and microstructural differences between C·Tr and P·Tr systems. The P·Tr beads served only as a rough reference, chosen principally because PS−DVB resins are more familiar to chemists involved in polymer-supported synthesis. From this perspective, we have demonstrated that C·Tr networks can provide ~30% higher effective dilution than conventional PS−DVB supports at the same loading.

Acknowledgment. This work was supported by the National Science Foundation, and we are grateful to Paul Bruins, University of California, Davis for his assistance during this project.

References and Notes

(1) Sherrington, D. C. In *Polymer Supported Reactions in Organic Synthesis*; Hodge, P., Sherrington, D. C., Eds.; Wiley: New York, 1980; p 67.
(2) Ford, W. T. In *Polymeric Reagents and Catalysts*; Ford, W. T., Ed.; American Chemical Society: ACS Symposium Series 308; Washington, DC, 1986.
(3) Crowey, J. I.; Rapoport, H. *Acc. Chem. Res.* **1976**, *9*, 135.
(4) Shea, K. J.; Thompson, E. A. *Macromolecules* **1985**, *18*, 814.
(5) Kurth, M. J.; Randall, L. A. A.; Chen, C. X.; *et al. J. Org. Chem.* **1994**, *59*, 5862.
(6) Kurth, M. J. *Chemia* **1996**, *50*, 261.
(7) Stein, A. D.; Hoffman, D. A.; Frank, C. W.; Fayer, M. D. *J. Chem. Phys.* **1992**, *96*, 3269.
(8) Oeser, R.; Ewen, B.; Richter, D.; Farago, B. *Phys. Rev. Lett.* **1988**, *60*, 1041.
(9) Rakshys, J. W., Jr. U.S.A. Patent No. 3,716,501, 1973.
(10) Lee, S.; Winnik, M. A.; Whittal, R. M.; Li, L. *Macromolecules* **1996**, *29*, 3060.
(11) Rozantzev, E. G.; Neiman, M. B. *Tetrahedron* **1964**, *20*, 131.
(12) Stewart, J. M.; Young, J. D. *Solid Phase Peptide Synthesis;* W. H. Freeman & Co.: San Francisco, 1969; p 55.
(13) Goldman, S. A.; Bruno, G. V.; Polnaszek, C. F.; Freed, J. H. *J. Chem. Phys.* **1972**, *56*, 716.
(14) *Spin Labeling: Theory and Applications*; Berliner, L. J., Ed.;, Academic Press: New York, 1976.
(15) Capiomont, A.; Chion, B.; Lajzerowicz, J.; Lemaire, H. M. *J. Chem. Phys.* **1974**, *60*, 2530.
(16) These were extrapolated from known values of a_n in various solvents and using a linear correlation between the Dimroth−Reichardt parameter ET(30) and a_n. This correlation has been shown to be valid for a number of nitroxides, including TEMPONE. See: Mukerjee, P.; Ramachandran, C.; Pyter, R. *J. Phys. Chem.* **1982**, *86*, 3189.
(17) Bales, B. L. In *Biological Magnetic Resonance*; Berliner, L. J., Reuben, J., Eds.; Plenum Press: New York, 1989; Vol. 8.
(18) Windle, J. J. *J. Magn. Reson.* **1981**, *45*, 432.
(19) Wang, F. W.; Lowry, R. E.; Grant, W. H. *Polymer* **1984**, *25*, 690.
(20) *Mechanisms of Photophysical Processes and Photochemical Reactions in Polymers*; Rabek, J. L., Ed.; John Wiley and Sons: Chinchester, 1987.
(21) LLharco, L. M.; Santos, A. M.; Silva, M. J.; Martinho, J. M. G. *Langmuir* **1995**, *11*, 2419.
(22) Cheung, S.-T.; Winnik, M. A.; Redpath, A. E. C. *Makromol. Chem.* **1982**, *183*, 1815.
(23) Winnik, M. A.; Li, X. B.; Guillet, J. E. *Macromolecules* **1984**, *17*, 699.
(24) Hu, H.; Horie, K.; Ushiki, H.; Tsunomori, F. *Eur. Polym. J.* **1993**, *29*, 1365.

(25) Winnik, M. A.; Redpath, A. E. C.; Richards, D. H. *Macromolecules* **1980**, *13*, 328.
(26) Birks, J. B. *Photophysics of Aromatic Molecules;* Wiley Interscience: New York, 1971.
(27) Wang, U.; Marawetz, H. *Makromol. Chem.* **1975**, *1*, 283.
(28) *Mechanisms of Photophysical Processes and Photochemical Reactions in Polymers;* Rabek, J. L., Ed.; John Wiley and Sons: Chinchester, 1987.
(29) Martinho, J. M. G.; Castanheira, E. M. S.; Reise e Sousa, A. T. *Macromolecules* **1995**, *28*, 1167.
(30) Phillips, D.; Roberts, A. J.; Soutar, I. *J. Polym. Sci., Polym. Lett. Ed.* **1980**, *18*, 123.
(31) Souter, I.; Phillips, D. In *Photophysical and Photochemical tools in Polymer Science*; Winnik, M. A., Ed.; NATO ASI Series 182; Reidel Publishing: Boston, 1986; p 97.
(32) It is reasonable that *Q* will be similar for labels bound to C·Tr and P·Tr, but the terms k_E and k_{-1} may vary for sites having different steric constraints. For simplicity, we assume these differences are small relative to the trends we are measuring.
(33) Winnik, M. A. *Photophysical and Photochemical Tools in Polymer Science*; Winnik, M. A., Ed.; Reidel Publishing: Boston, 1986; pp 293−324.
(34) Cuniberti, C.; Perico, A. *Eur. Polym. J.* **1980**, *16*, 887.
(35) Shea, K. J.; Stoddard, G. T. *Macromolecules* **1991**, *24*, 1207.
(36) Harwood, H. J. In *Reactions on Polymers*; Moore, J. A., Ed.; Reidel: Boston, 1973; p 188.
(37) Farid, S.; Martic, P. A.; Daly, R. C.; Thompson, D. R.; Specht, D.; Hartman, S. E.; Williams, J. L. R. *Pure Appl. Chem.* **1979**, *51*, 241.
(38) The dry polymers (loading ∼ 0.17 mmol/g) did not exibit excimer fluorescence at room temperature, but upon heating in an oil bath at 100 °C for 30 s, excimer emission was observed.
(39) Bastide, J.; Boue, F.; Buzier, M. In *Molecular Basis of Polymer Networks;* Braumgartner, A.; Picot, C. E., Eds.; Springer-Verlag: Berlin, 1989.
(40) Erman, B.; Flory, P. J. *Macromolecules* **1982**, *15*, 806.
(41) Stevens, B.; Ban, M. I. *Trans. Faraday Soc.* **1964**, *60*, 1515.
(42) Warshel, A.; Huler, E. *Chem. Phys.* **1974**, *6*, 463.
(43) Bohne, C.; Konuk, P.; Scaiano, J. C. *Chem. Phys. Lett.* **1988**, *152*, 156.
(44) Oyama, H. T.; Hemker, D. J.; Frank, C. W. *Macromolecules* **1989**, *22*, 1255.
(45) *Encyclopedia of Polymer Science and Engineering*; John Wiley & Sons: New York, 1984; Vol. 16, p 67.
(46) Stone, T. J.; Buckman, T.; Nordio, P. L.; McConnell, H. M. *Proc. Natl. Acad. Sci. U.S.A.* **1965**, *54*, 1010.
(47) Wasserman, A. M.; Buchachenko, A. L.; Kovarskii, A. L.; Neiman, M. B. *Eur. Polym. J.* **1969**, *5*, 473.
(48) Tormala, P.; Lattila, H.; Lindberg, J. J. *Polymer* **1973**, *14*, 481; *Angew. Makromol. Chem.* **1974**, *37*, 135.
(49) Chesnut, D. B.; Hower, J. F. *J. Phys. Chem.* **1971**, *75*, 907.
(50) Veksli, Z.; Miller, W. G. *Macromolecules* **1974**, *8*, 248.
(51) Regen, S. L. *J. Am. Chem. Soc.* **1974**, *96*, 5275.
(52) Tormala, P.; Lindberg, J. J. In *Structural Studies of Macromolecules by Spectroscopic Methods*; Ivan, K. J., Ed.; Wiley-Interscience: London, 1976.
(53) Millhauser, G. L.; Fiori, W. R.; Miick, S. M. In *Methods in Enzymology*; Sauer, K., Ed., Academic Press: New York, 1995; Vol. 246.
(54) Bullock, A. T.; Cameron, G. G.; Smith, P. M. *J. Chem. Soc., Faraday Trans. 2* **1974**, *70*, 1202.
(55) Goldenberg, M.; Emert, J.; Marawetz, *H. J. Am. Chem. Soc.* **1978**, *100*, 7171.

MA961578P